

NASA TM X-638

GPO PRICE \$

CFSTI PRICE(S) \$

Hard copy (HC) \$150

Microfiche (MF) 150

1963 July 67

Copy

27

NASA TM X-638



TECHNICAL MEMORANDUM

X-638

PRELIMINARY RESULTS OF AERODYNAMIC HEATING STUDIES

ON THE X-15 AIRPLANE

By Richard D. Banner, Albert E. Kuhl,
and Robert D. Quinn

Flight Research Center
Edwards, Calif.

DECLASSIFIED
ATS 480

AUTHORITY
DROBKA TO LEBOW
MEMO DATED 12/13/6

Declassified by authority of NASA
Classification Change Notices No. 43
Dated ** 12/29/65



N66 29468

(ACCESSION NUMBER)

(THRU)

(PAGES)

700X-638
(NASA CR OR TMX OR AD NUMBER)

(CODE)

(CATEGORY)

FACILITY FORM 602

NATIONAL AERONAUTICS AND SPACE ADMINISTRATION

WASHINGTON

March 1962



1J

DECLASSIFIED

AUTHORITY
DROBKA TO LEBOW
MEMO DATED 12/13/6


NATIONAL AERONAUTICS AND SPACE ADMINISTRATION

TECHNICAL MEMORANDUM X-638

PRELIMINARY RESULTS OF AERODYNAMIC HEATING STUDIES

ON THE X-15 AIRPLANE* **

By Richard D. Banner, Albert E. Kuhl, and Robert D. Quinn

DECLASSIFIED
ATS 480

SUMMARY

29468

The results of the preliminary flight heat-transfer studies on the X-15 airplane are presented, together with a discussion of the manner in which the data have been obtained, a comparison of measured and calculated turbulent heat-transfer coefficients, a correlation of the model test results and the flight results for turbulent heat transfer, some information on boundary-layer transition, and a comparison of measured and calculated skin temperatures at several locations on the airplane.


INTRODUCTION

One of the primary purposes of the X-15 program is the measurement and analysis of the aerodynamic heating of the airplane in actual flight. In the course of expanding the performance and altitude capabilities of the airplane, a considerable amount of heating data in the form of measured temperature has been obtained. These data, together with simplified calculations, have been used to define a safe operational environment for the airplane. For certain flight conditions the temperature data have been used to obtain heat-transfer coefficients and have been compared with the results of model tests and prediction methods.

Because of the discrepancies between the various turbulent heat-transfer methods, designers attempt to choose a conservative approach. The heat-transfer data obtained in the X-15 model tests, together with flight-test data of the airplane, provide a means of assessing the adequacy of current aerodynamic heat-transfer design procedures.

*This document is based on a paper presented at the Conference on the Progress of the X-15 Project, Edwards Air Force Base, Calif., November 20-21, 1961.

**Title, Unclassified.

 Declassified by authority of NASA
Classification Change Notices No. 43
Dated **12/29/65

H
2
3
4

SYMBOLS

c_p	specific heat, $\frac{\text{Btu}}{\text{lb-}^\circ\text{F}}$
H	altitude, ft
h	heat-transfer coefficient, $\frac{\text{Btu}}{\text{ft}^2\text{-}^\circ\text{F-sec}}$
M	Mach number
N_{Pr}	Prandtl number
N_{St}	Stanton number, $\frac{h}{\rho_l V_l c_p}$
$N_{St,i}$	incompressible Stanton number $\left(\text{by Blasius theory, } \frac{0.0296}{(N_{Pr})^{2/3} (R_l)^{1/5}}; \text{ reduced experimental data, } N_{St} \left[\frac{(T^*)_{aw}}{T_l} \right]^{.65} \right)$
p	pressure
$P_{t,A}$	attached-shock total pressure
$P_{t,N}$	total pressure behind normal shock
$P_{t,\infty}$	free-stream total pressure
R	Reynolds number, $\frac{\rho V x}{\mu}$
T	temperature, $^\circ\text{F}$ or $^\circ\text{R}$
T^*	reference temperature, $T^* = T_l + 0.5(T_w - T_l) + 0.22(T_R - T_l)$
$(T^*)_{aw}$	adiabatic-wall reference temperature, $(T^*)_{aw} = T_l + 0.72(T_R - T_l)$
T_R	boundary-layer recovery temperature, $T_R = T_l \left(1 + \frac{\gamma - 1}{2} \eta M_l^2 \right)$
V	velocity, ft/sec
x	length, ft



- x_f length from fuselage nose, ft
- x_w length from wing leading edge, ft
- α angle of attack, deg
- γ ratio of specific heats
- δ_{SB} speed-brake deflection
- η recovery factor ($\sqrt{N_{Pr}}$ for laminar flow, $\sqrt[3]{N_{Pr}}$ for turbulent flow)
- μ coefficient of viscosity, lb/ft-sec
- ρ density, lb/cu ft

Subscripts:

- l local
- w wall or skin
- ∞ free stream

INSTRUMENTATION

The number and location of surface thermocouples and static-pressure orifices for the X-15 flight tests are shown in figure 1. There are 293 surface thermocouples on the airplane. The thermocouples are 30-gage chromel-alumel wires, spot-welded to the inside surface of the skin. There are 136 surface-pressure orifices. The static-pressure taps are 5/16-inch outside-diameter tubing installed flush with the outside surface of the skin. Both the thermocouple wires and the tubes are connected to onboard recording instruments in the fuselage of the aircraft.

The instrumentation is primarily located on the right-hand side of the airplane; however, there are corresponding measurements on the left-hand side of the forward fuselage and the midsemispan station of the vertical tail. No instrumentation is located in the vicinity of the liquid-oxygen and fuel tanks, which are integral tanks. The instrumentation on the wing is primarily located at three spanwise stations, both top and bottom. On the top and bottom of the horizontal tail, only thermocouples have been installed.

Although temperature data have been obtained during all X-15 flights at most of the locations shown in figure 1, relatively few flights have met the requirements for accurate reduction of heat-transfer data by the transient-skin-temperature procedure. Transient analysis requires high skin-heating rates and low skin temperatures, while relatively constant flight conditions are maintained.

TEST CONDITIONS

Two types of flights which are of interest in the aerodynamic heating study are shown in figure 2. The maximum speed for both flights was near 5,000 feet per second. The flight shown on the left attained a relatively low altitude, near 100,000 feet. Heat-transfer-coefficient data were obtained from the skin heating rates during a period of time (shown by the shaded strip) when velocity, altitude, and angle of attack were relatively constant and when the skin temperature was increasing at a rapid rate. The flight shown on the right in figure 2 is typical of many high-altitude flights during which the velocity, altitude, and angle of attack are changing quite rapidly; for this reason heat-transfer-coefficient data are not reduced. However, the heat transfer during high-altitude flights can sometimes be inferred from comparisons of calculated and measured skin temperatures.

Flight heat-transfer data have been obtained at Mach numbers near $M_{\infty} = 3, 4, \text{ and } 5$. During the design of the X-15, heat-transfer tests were conducted on a 1/15-scale model of the X-15, and turbulent heat-transfer data were obtained at Mach numbers of $M_{\infty} = 3, 4.65, \text{ and } 7$. Both the model test conditions and the present flight-test conditions are shown in figure 3 in terms of the parameters which affect heat transfer. Also shown is the variation in the heat-transfer parameters that is obtained from the X-15 design speed and altitude flight missions. (The Reynolds numbers and wall, or skin, temperatures have been based upon a location 1 foot behind the wing leading edge.)

As is frequently the case, the X-15 design flight conditions were outside the range of the wind-tunnel test conditions, and it was necessary to extrapolate the turbulent heat-transfer data on the model, obtained at relatively low Reynolds numbers and heating rates, to the Reynolds numbers and heating rates of the flight conditions.

METHODS

The difficulty in extrapolating turbulent heat-transfer data, as well as in predicting the actual level, is illustrated in figure 4. At

the lower Mach number, Eckert's reference-temperature method (ref. 1) and the theory of Van Driest (ref. 2) tend to agree better than at the higher Mach number. At both Mach numbers, however, the reference-temperature method indicates a lower level at the adiabatic-wall condition and a greater increase in heat transfer with increased heating (lower values of T_w/T_R) than does the theory of Van Driest.

Some recent results of a study by Winkler (ref. 3) indicate about the same level of heat transfer as the reference-temperature method at the adiabatic-wall condition but show a decrease with increasing rate of heat transfer, which is opposite to the behavior predicted by the other theories and empirical methods. Winkler interprets the results as confirmation of data previously obtained (ref. 4). The data of reference 4 were generally discounted by Sommer and Short in their development of the T' method (ref. 5).

One of the primary difficulties in the analysis of turbulent heat-transfer data is the determination of the conditions to be used in the flat-plate equations based on the flow properties at the boundary-layer edge. In this regard, the X-15 data, presented herein, have been based upon the assumption that the flow properties at the boundary-layer edge (behind leading-edge regions) can be calculated by conventional attached-shock methods (ref. 6). The adequacy of this assumption is discussed in the next section.

DISCUSSION OF RESULTS

Surface Pressures and Heat Transfer

Surface-pressure and heat-transfer-coefficient data have been obtained during low angles of attack for free-stream Mach numbers near 3, 4, and 5, and at altitudes of less than 100,000 feet. For the most part, the flow has been turbulent. The surface pressures and heat transfer which have been measured on the lower wing surface about midsemispan and on the lower-fuselage centerline at a free-stream Mach number of about 4 and at an angle of attack of about 4° are shown in figure 5. In the upper part of the figure measured pressures are compared with calculated pressures, and in the lower part of the figure measured heat-transfer data are compared with calculations. For the wing, the surface pressures are closely estimated by assuming an attached shock and expanded flow over the wing. Similarly, good agreement is shown for the lower fuselage centerline, where a tangent-cone approximation has been used to calculate the local pressure levels. Calculation of the turbulent heat transfer is not so straightforward, however, since, in addition to the local static-pressure level, some idea of the local total pressure is required. The estimation of a local total pressure is somewhat involved, since an

CONFIDENTIAL

understanding of the entropy change along a streamline is required. In lieu of this information, the total-pressure level can be bracketed between the free-stream total pressure and the total pressure that would exist behind a specified number of shocks. When the limiting local flow conditions have thus been established and a choice of a turbulent heat-transfer method has been made, local heat-transfer coefficients can be calculated.

The calculations shown in figure 5 as the upper and lower boundaries of the shaded areas represent the heat-transfer coefficients that would be calculated when Eckert's reference-temperature method is used, together with the measured static pressures and the assumption of the free-stream total pressure and the total pressure behind a normal shock. The assumption of free-stream total pressure overestimates the measured levels of turbulent heat transfer by 50 to 60 percent. The assumption of a total-pressure level equal to that behind a normal shock overestimates the measured data by 15 to 25 percent.

H
2
3
4

Shown by the solid line in figure 5 are calculated heat-transfer coefficients which have been obtained by assuming the calculated static pressure, the total pressure that is calculated behind the attached shock, and neglecting the effect of heating rate on the heat-transfer coefficient. This approach overestimates the measured data by 10 to 20 percent. Neglecting the effect of heating rate in the calculation of the heat-transfer coefficient is accomplished by substituting the boundary-layer recovery temperature for the skin temperature in the equation used to calculate the reference temperature. The result is interpreted as an adiabatic-wall reference temperature and accounts only for the effects of compressibility on the heat transfer. The attached-shock total pressure was used, since it is believed that it is a better approximation than either the free-stream or the normal-shock total pressure. Whether this approach can be generalized depends largely on subsequent measurements of the actual total-pressure levels in flight over a range of skin heating rates. The simplicity afforded by this approach and the favorable agreement that has been obtained has resulted in the choice of this method for computing the local levels of turbulent heat transfer.

This approach has also been chosen to illustrate the correlation between flight-test data and the model data which were obtained at different Reynolds numbers and heating rates. The correlation is shown in figure 6. Flight data, obtained at free-stream Mach numbers of 3, 4, and 5, and model data, obtained at a Mach number of 3, have been reduced by the adiabatic-wall reference-temperature method to the incompressible value of the dimensionless heat-transfer coefficient, the Stanton number, divided by the local Reynolds number to the 0.8 power and are shown plotted against the local Reynolds number. In this manner, the flat-plate theory now corresponds to the solid lines shown, and the data obtained at various Mach numbers and local Reynolds numbers can be shown

CONFIDENTIAL

DECLASSIFIED

7

for comparison. For the lower wing surface, both the flight data and the model data are correlated fairly well over the Reynolds number range of the tests. For the forward fuselage, the dashed line represents a 15-percent increase over the flat-plate theory to allow for conical flow. Most of the flight data correlate fairly well over the Reynolds number range, and the use of a conical transformation results in slightly conservative estimates. The model data, which were obtained at a free-stream Mach number of 3 and an angle of attack of zero on the side of the fuselage, seem to agree favorably. The bottom fuselage data on the model, however, are from 50 to 100 percent higher than the remainder of the data. This result is thought to be caused by roughness effects, since sand-grain roughness was applied on both sides of the model bottom centerline in order to trip the boundary layer and assure turbulent flow at angles of attack.

The model data was used by the manufacturer to determine empirical factors that would correct flat-plate heat-transfer coefficients to those computed from the model data. These same factors were incorporated in computed programs to correct heat-transfer coefficients computed for the full-scale airplane flying assigned missions. It is interesting to note that if the theory is adjusted to fit the model bottom centerline data and the results are extrapolated to the flight Reynolds number range, a considerable overestimate of the flight heat transfer is obtained.

Boundary-Layer Transition

A particular area of interest in the flight results is boundary-layer transition. At present, two methods are used to detect laminar and turbulent areas on the airplane in flight. The first, of course, is the thermocouple data reduced to heat-transfer coefficients, which show a much higher level of heat transfer in a turbulent boundary layer than in a laminar boundary layer. The second is in the use of temperature-sensitive paints which are applied to large surface areas of the airplane prior to a flight.

How these methods are used and an illustration of the type of transition that has been detected on the X-15 is shown in figure 7. In the upper right is a postflight photograph of the lower surface of the X-15 wing, which had been coated with temperature-sensitive paint prior to flight. This wing is opposite the heavily instrumented wing. The line on the photograph shows the corresponding location of the midespan thermocouple row. The postflight temperature-paint patterns indicated high-temperature, wedge-shaped areas originating at leading-edge expansion joints and extending a considerable distance rearward. The surface discontinuities of the expansion joints, which are rather severe, apparently produce turbulent flow during the entire flight and lead to higher temperatures in the wedge-shaped areas.

CONFIDENTIAL

An example of the measured heat-transfer data which seem to substantiate this analysis is shown in the lower portion of figure 7. Two independent sets of data are shown for a Mach number of about 4 and an angle of attack of about 4° . The data shown by the circular symbols are for the normal leading edge of the wing with expansion joints. The data shown by the square symbols were obtained with the boundary layer artificially tripped at the leading edge immediately ahead of the thermocouple station. The data that were obtained with the normal leading edge show an abrupt increase in the heat transfer from a laminar level to a turbulent level at a distance of about 1.2 feet from the leading edge. This distance corresponds approximately to the point where the lateral spread of turbulence originating at the leading-edge joint would cross the thermocouple station. From this point rearward the turbulent level of heat transfer is about the same as that for the all-turbulent case, and both sets of data appear to be fairly well predicted by the turbulent method discussed previously.

H
2
3
4

Since these data were obtained, small shields (fig. 8) have been used to cover the leading-edge expansion joint and thus to reduce the severity of the surface discontinuity. Recent tests with the shields installed still show the wedge-shaped patterns in the temperature paints, although it is believed that the length of time during a flight that the turbulent wedges exist has been reduced. It should be pointed out that the light areas shown in the photograph of the wing (fig. 7) do not necessarily imply laminar flow, but, rather, that these areas were at least not all turbulent during the flight.

Boundary-layer transition, which may be produced by such discontinuities in the surface of a high-speed vehicle, would be extremely difficult to predict. As yet, for the X-15, a parametric correlation has not been established which would allow the prediction of the transition location on the wing a priori. Under these circumstances, it would seem that conservative estimates of transition should still be required.

Skin Temperatures

In order to compare measured skin temperatures with predicted values, based on the turbulent heat-transfer correlation presented earlier, and to illustrate how boundary-layer transition during flight affects the resulting skin temperature, figure 9 shows measured and calculated temperatures for a point on the wing during both the low- and high-altitude flights. This location is on the lower surface of the wing, about midsemispan, and is 1.4 feet from the leading edge. For the low-altitude flight, the measured data indicate all-turbulent flow at this point, since a fairly high skin heating rate and maximum temperature were experienced. The calculated turbulent skin temperature

CONFIDENTIAL

agrees well during the high heating period but slightly overestimates the measured value near its peak and during a period of cooling just following the peak temperature. A close look at the trajectory (fig. 2) indicates a fairly high angle of attack during this period, and the differences in the measured and calculated temperatures may be due to the inability to predict the local flow conditions properly during this period of time.

For the high-altitude flight, this point on the wing appears to be experiencing some laminar flow. An all-turbulent calculation results in a higher temperature than was measured during the exit phase of the trajectory, greater cooling during the ballistic portion, and an overestimate of the maximum temperature that was experienced during the reentry. The assumption of laminar flow during the latter part of the exit phase and the ballistic portion of the trajectory results in better agreement between the measured and calculated data. This location on the wing is felt to be affected by the previously discussed turbulent wedge, which originates at the leading edge. Exactly what causes this location to go laminar at the higher altitudes is not known, but it is possible that the turbulent wedge either vanishes or that its lateral spread is delayed.

It appears that when the boundary layer is known to be either laminar or turbulent, the skin temperature can be predicted with reasonable accuracy. This statement seems to apply also to other areas of the airplane. Flow on the fuselage, for example, seems to be turbulent over the entire length, at least for the relatively low angles of attack that have been experienced. In discussing the fuselage temperatures, it is of interest to look first at typical temperature measurements that have been obtained near the stagnation region of the fuselage, which is the area of the high-speed flow-direction sensor. These data are shown in figure 10.

The sensor is 6.5 inches in diameter, spherically shaped, and heat-sink constructed. An orifice is located at the stagnation point and measures the stagnation pressure. Four other orifices are located about 40° from the stagnation point in the vertical and horizontal planes and measure differential pressures. A servo system nulls the sensor in the free-stream direction.

Thermocouples have been installed on the inside surface of the sensor at various angular positions. Measured data which were obtained during the high-altitude flight at locations 20° and 80° from the stagnation point are shown by the symbols. The measured temperatures at the 20° location are 200° to 250° higher than at the 80° location. In order to calculate the inside surface temperatures, a spherical segment of the sensor was divided into small lumps and the conduction

and convective heat-transfer problem was simulated in a digital computer. Newtonian pressures with isentropic expansion and Lees' laminar theory were used to obtain the aerodynamic-heating input; the resulting calculated temperatures are shown by the solid lines. Good agreement is shown for the calculated and measured values at the 20° location, but the measured values at the 80° location are considerably higher than the calculations. Significant differences are noted between the measured and calculated heating rates at the 80° location during the early part of the exit phase and during the reentry, which suggests that the high heating at the 80° location is associated with high Reynolds numbers. There are several possible reasons why heating at the 80° location is higher than would be expected. First, there may be turbulence induced by the upstream pressure orifice at this location; secondly, the proximity of the lip on the assembly may create either a stagnant region or separated flow; or, the cause may be a combination of these phenomena. Some early wind-tunnel tests of a similar configuration at the Langley Research Center had shown that high heating could be expected on the assembly lip itself, but the results that are presently being experienced in flight were not evident in the tunnel tests. The higher heating in this region has not caused any alarm, nor is it expected to, since cooling has been provided for the assembly in the event it is required.

H
2
3
4

The surface discontinuity presented by the assembly lip seems sufficient to trip the boundary layer to turbulent flow, if it is not already turbulent, since most of the heat-transfer and skin-temperature data that have been obtained on the fuselage have been at the turbulent level. Evidence of this is presented in figure 11, in which measured skin temperatures are compared with calculated values for the low-altitude flight. In addition, similar comparisons are made for the lower speed brake, which also seems to be in an all-turbulent area.

On the forward-fuselage lower centerline, the measured temperature data are shown for a point 11 feet behind the nose. The solid line represents calculated values based on tangent-cone static and total pressures and the adiabatic-wall reference temperature. The calculated temperatures agree fairly well with the measured data, although they are slightly high near and just following the peak temperature, where higher angles of attack were experienced during the flight.

The speed brake provides another interesting area for comparisons to be made, since the use of such a high-drag device is intended to reduce the overall heating of the airplane during reentry flight, as well as to provide increased directional stability. The measured skin temperature is shown in figure 11 for a point near the rear of the speed brake. For the flight shown, the speed brake was deflected 35° at time 80 seconds. Model data indicated that with the speed brake deflected, the heat transfer could be closely estimated if the flow length were chosen from the hinge line. The calculation labeled x₁ is

CONFIDENTIAL

DECLASSIFIED

11

based on this assumption and is seen to overestimate the maximum measured temperature about 100°. For comparison, temperatures have been calculated based on the flow length from the leading edge, and the values labeled x_2 are seen to estimate the measured values more closely. The ratio of these two lengths would indicate a 25-percent reduction in the level of heat transfer when the distance from the leading edge is used. As a matter of interest, a calculation is shown for the speed brake undeflected, which, when compared with the measured data, indicates a 500° temperature rise on the speed brake due to its use during the flight.

CONCLUDING REMARKS

Heat-transfer data have been obtained on the X-15 in flight to speeds near free-stream Mach numbers of 3, 4, and 5, and at relatively low angles of attack. Turbulent heat-transfer methods are reviewed and compared with the X-15 flight data. The level of heat transfer predicted by the reference-temperature method, which accounts for the effect of heating rate, is from 15 to 60 percent higher than the measured data, depending upon the assumed total-pressure level. Closer agreement with the measured data was obtained when the effect of heating rate was neglected and attached-shock total-pressure levels were used. Some evidence of the manner in which boundary-layer transition takes place on the airplane in flight has been shown, and the results suggest the advisability of continuing to use conservative estimates for the transition location.

Flight Research Center
National Aeronautics and Space Administration
Edwards, Calif., November 20, 1961

03:15:30:030

12

REFERENCES

1. Eckert, Ernst R. G.: Survey on Heat Transfer at High Speeds. WADC Tech. Rep. 54-70 (Contract No. AF 33(616)-2214, RDO No. 474-143), Wright Air Dev. Center, U.S. Air Force, Apr. 1954.
2. Van Driest, E. R.: The Problem of Aerodynamic Heating. Aero. Eng. Rev., vol. 15, no. 10, Oct. 1956, pp. 26-41.
3. Winkler, Eva M.: Investigation of Flat Plate Hypersonic Turbulent Boundary Layers With Heat Transfer. [Preprint] 856-59, American Rocket Soc., June 1959.
4. Lobb, R. K., Winkler, Eva M., and Persh, Jerome: NOL Hypersonic Tunnel No. 4 Results VII: Experimental Investigation of Turbulent Boundary Layers in Hypersonic Flow. NAVORD Rep. 3880, U.S. Naval Ord. Lab. (White Oak, Md.), Mar. 1, 1955.
5. Sommer, Simon C., and Short, Barbara J.: Free-Flight Measurements of Turbulent-Boundary-Layer Skin Friction in the Presence of Severe Aerodynamic Heating at Mach Numbers From 2.8 to 7.0. NACA TN 3391, 1955.
6. Ames Research Staff: Equations, Tables, and Charts for Compressible Flow. NACA Rep. 1135, 1953. (Supersedes NACA TN 1428.)

H
2
3
4

[REDACTED]

H-234

X-15 AIRPLANE SURFACE INSTRUMENTATION

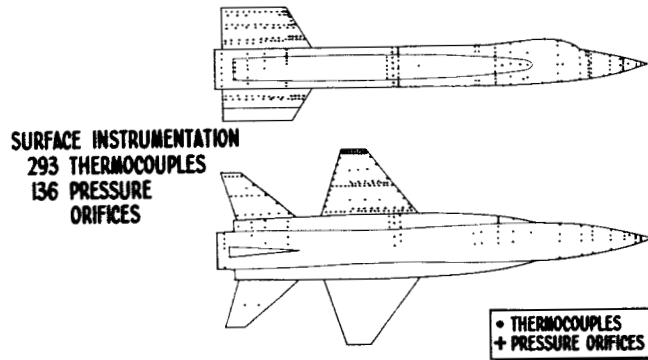


Figure 1

TYPICAL HEATING FLIGHTS

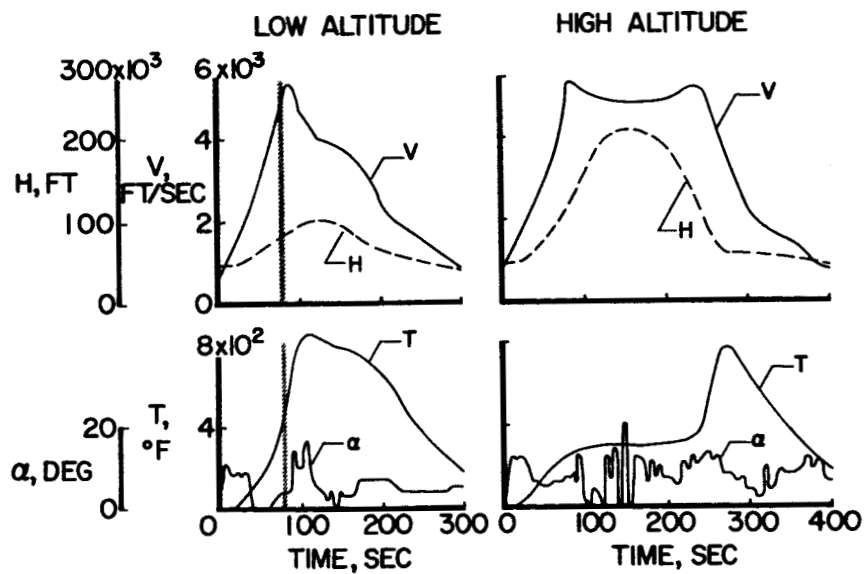
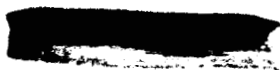


Figure 2



HEAT-TRANSFER TEST CONDITIONS

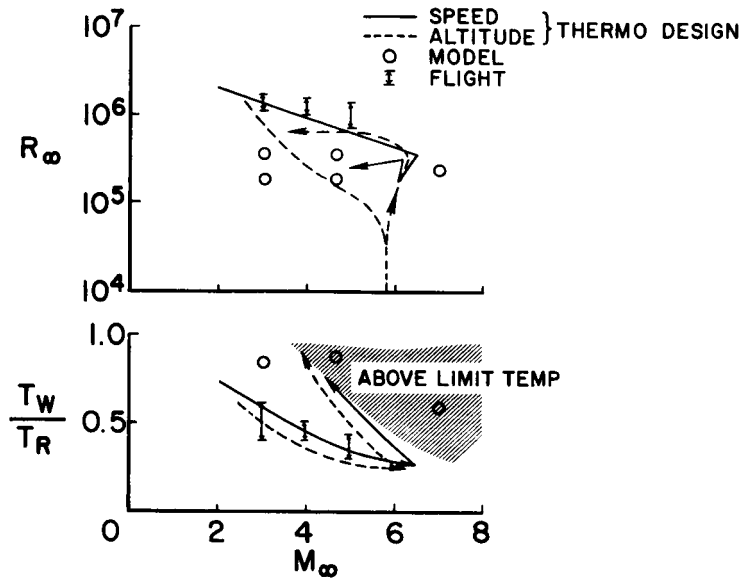


Figure 3

TURBULENT HEAT-TRANSFER METHODS

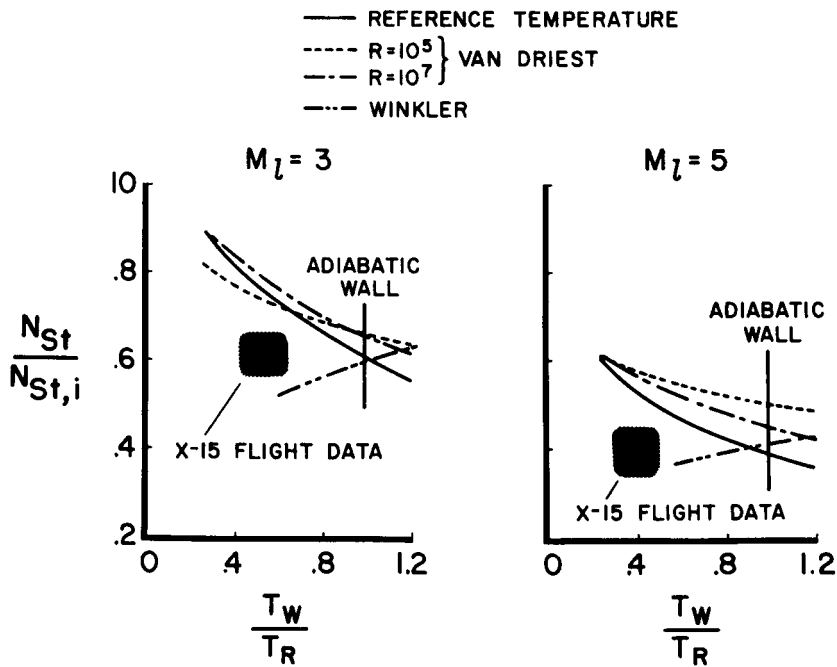


Figure 4

H-234

H-234

SURFACE PRESSURES AND HEAT TRANSFER

$M_{\infty} \approx 4, \alpha \approx 4^{\circ}$

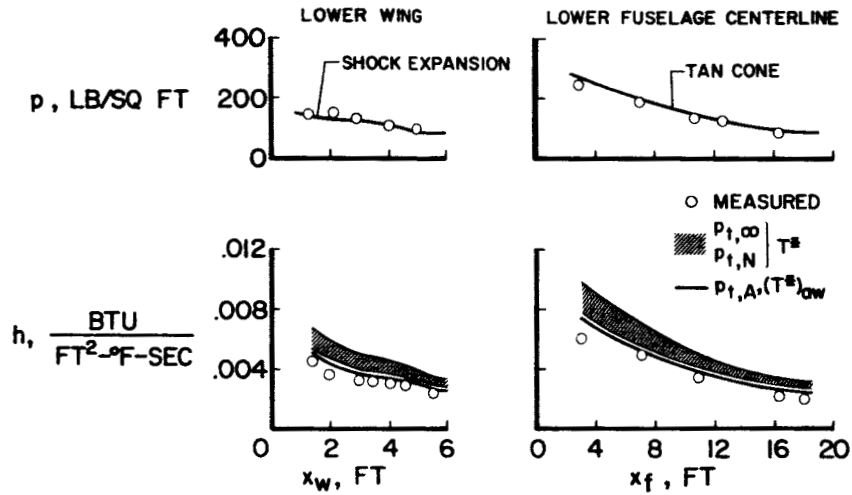


Figure 5

REYNOLDS NUMBER CORRELATION

ADIABATIC REFERENCE TEMPERATURE

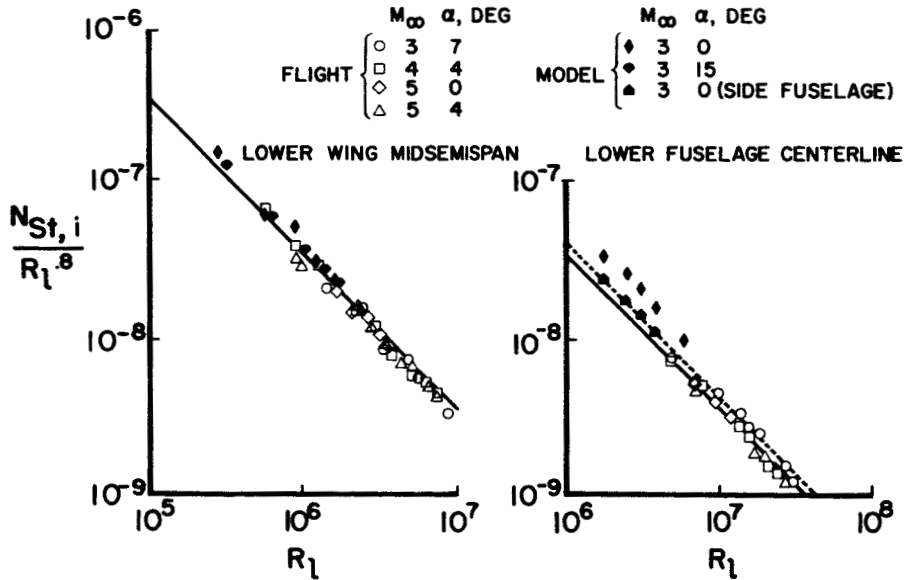


Figure 6



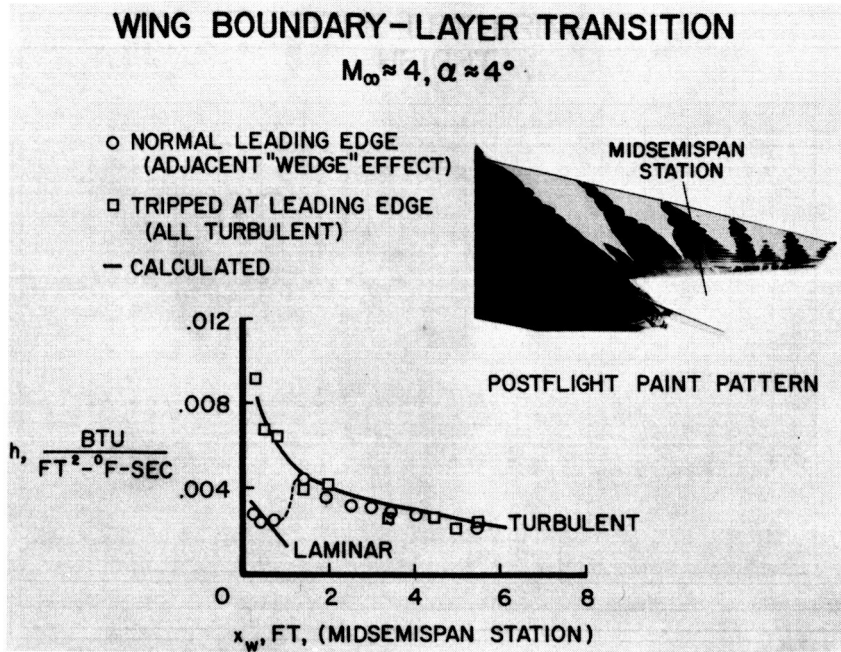


Figure 7

WING LEADING-EDGE EXPANSION JOINTS

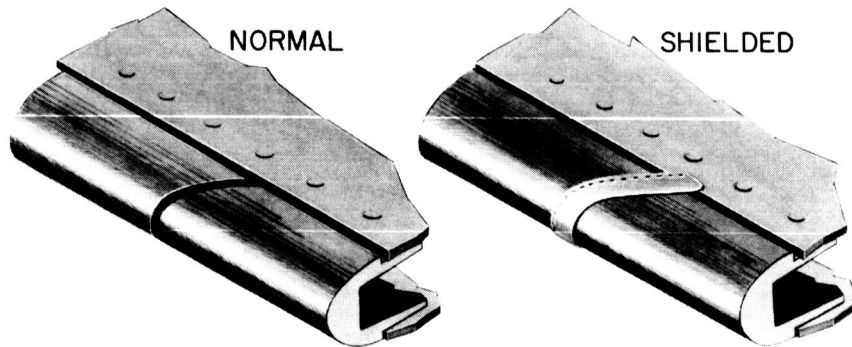


Figure 8

WING SKIN TEMPERATURES

$x_w=1.4$ FT, LOWER MIDSEMPAN

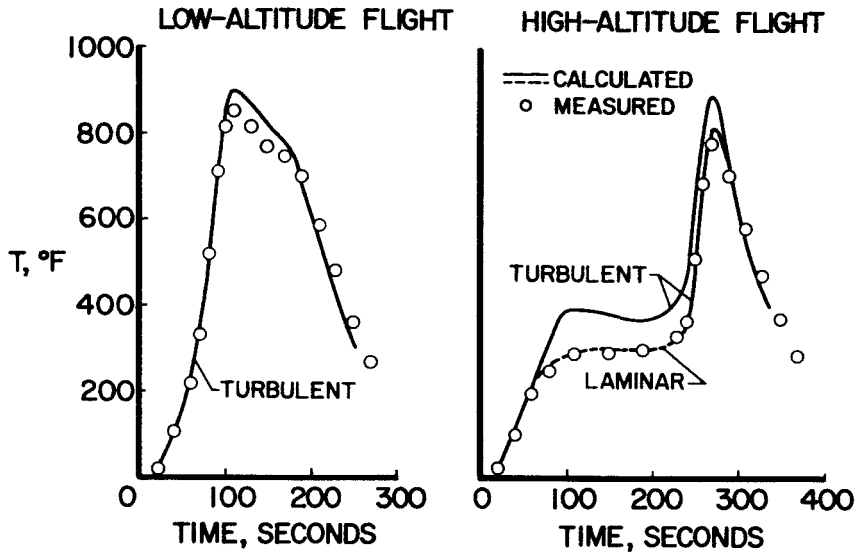


Figure 9

FLOW-DIRECTION-SENSOR TEMPERATURES HIGH-ALTITUDE FLIGHT

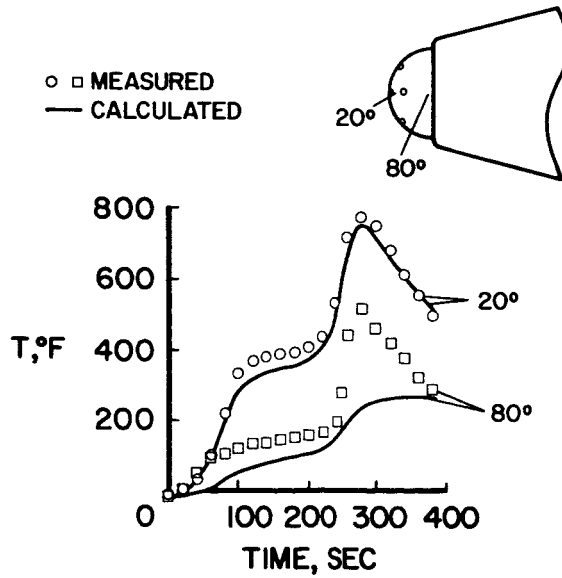


Figure 10

H-234



SKIN TEMPERATURES IN TURBULENT AREAS LOW-ALTITUDE FLIGHT

○ MEASURED
— CALCULATED

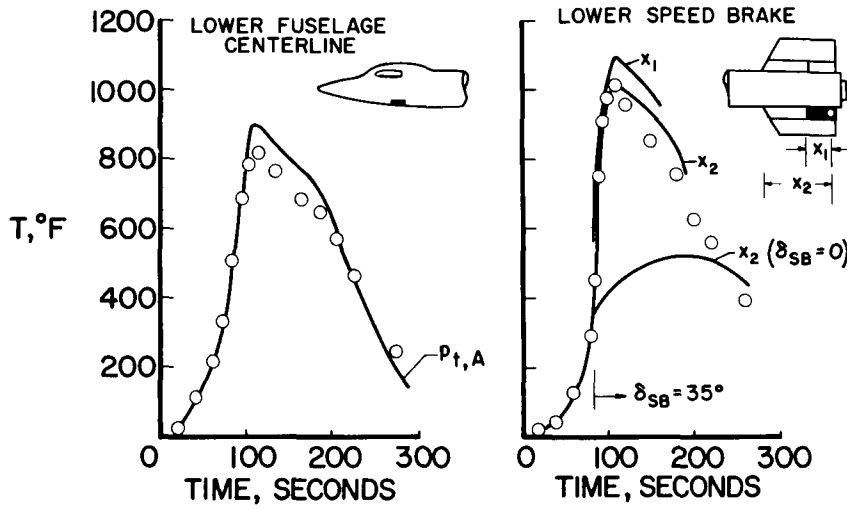


Figure 11